RSC Advances

ROYAL SOCIETY OF CHEMISTRY

www.rsc.org/advances

Title

Crystal Chemical Investigation of Nano Inclusion in $LiMn_2O_4$ Cathode Material of Lithium Ion Battery

Author

Shogo Esaki,[a,b] Motoaki Nishijima,[b] Shigeomi Takai,[a] and Takeshi Yao[*c,d]

Affiliation

1 Department of Fundamental Energy Science, Graduate School of Energy Science, Kyoto University,

2 Materials and Energy Technology Laboratories, Corporate Research and Development Group, SHARP CORPORATION,

3 Kagawa National College of Technology

4 Institute of Advanced Energy, Kyoto University

Address

1 Yoshida, Sakyo-ku, Kyoto 606-8501, Japan

2 2613-1, Ichinomoto-cho, Tenri, Nara 632-8567, Japan

3 335 Chokushi-cho, Takamatsu, Kagawa 761-8058, Japan

4 Gokasho, Uji, Kyoto 611-0011, Japan

* Corresponding author

Abstract

In this study, $LiMn_2O_4$ was fabricated with "Nano Inclusions" and the detailed crystal structure of the sample was studied by HAADF-STEM observation with an electron beam tilted to the specimen, electron diffraction, HRTEM observation. HAADF-STEM observation and electron diffraction revealed that the "Nano Inclusions" were located within single $LiMn_2O_4$ crystals. HRTEM observation clarified that the (100) plane of $LiMn_2O_4$ and the (110) plane of $ZnMn_2O_4$ have a common cubic close-packed oxygen arrangement and connect to each other without forming grain boundaries, due to similar atomic arrangements of $LiMn_2O_4$ along the <100> direction and of $ZnMn_2O_4$ along the [110] and [$1\bar{1}0$] direction.

Introduction

$LiMn_2O_4$ with a cubic spinel structure has been widely studied as a cathode material for lithium ion batteries because of its nontoxicity, availability, low cost and safety. However, $LiMn_2O_4$ suffers from severe capacity fading during charge and discharge cycles. Many trials have been investigated for improving the cycle performance such as by substitution[1-12] of Mn with other elements to restrain the phase transition and to stabilize the crystal structure, surface modification[13-17] of $LiMn_2O_4$ with other compounds to protect Mn from dissolution, stabilizing[18,19] $LiMn_2O_4$ spinel crystal lattices with other spinel crystals inert to electrochemical reaction thorough common oxide ion

arrangements.

Recently, we reported a novel improvement of the cycle performance for $LiMn_2O_4$ by using "Nano Inclusions". [20] We added Zn_2SnO_4 to the Li_2CO_3 and MnO_2 mixtures with a molar ration of Li : Mn = 1 : 2, and calcined and fired the mixture. As a result, within the $LiMn_2O_4$ single crystals, nano-scale thin plate-shaped $ZnMn_2O_4$ crystals were induced, which we named "Nano Inclusions" after the similar characteristics of "inclusions" in mineralogy and their nano scale. "Nano Inclusions" suppressed crack propagation caused by volume changes during the charge and discharge process and prevented dead region formation, which causes the capacity decrease. [21-24] The discharge capacity retention rates at the 100th cycle increased from 0.862 for $LiMn_2O_4$ to 0.992 for x = 0.05 in (1-x)$LiMn_2O_4$-$x$$Zn_2SnO_4$ for example. The cycle performance of $LiMn_2O_4$ with "Nano Inclusions" was superior to that of $LiMn_2O_4$ without it.

In this study, we conducted the crystal chemical investigation of "Nano Inclusions" in $LiMn_2O_4$.

Experimental

$LiMn_2O_4$ samples were prepared with "Nano Inclusions" denoted as (1-x)$LiMn_2O_4$-$x$$Zn_2SnO_4$ (x = 0, 0.02, 0.05) using the same method as our previous study. [20] Observation of the cross section for the samples was studied by using high-angle annular dark-field

scanning transmission electron microscopy (HAADF-STEM, HF-2210, Hitachi, Ltd. Japan) at an accelerating voltage of 200 kV. Additionally, detailed HAADF-STEM observations were carried out with electron beams tilted to the sample. Electron diffraction patterns with the electron beam spot size 0.7 nm were measured to study the crystal orientation. High-resolution transmission electron microscopy (HRTEM) were carried out to clarify the atomic arrangement of $LiMn_2O_4$ and "Nano Inclusions".

Results and discussion

Figure 1 shows HAADF-STEM cross section images of the samples. The particles of $LiMn_2O_4$ were observed. White lines were observed within the particles for x = 0.02 and 0.05. The width of the white lines were in the range of a few tens of nanometers. These white lines are "Nano Inclusions".

HAADF-STEM observation images with electron beam tilted to the specimen for the sample of x = 0.05 are shown in Figure 2. When one "Nano Inclusion" indicated by a white arrow in the figure is paid attention to as an example, it was line-shaped at -36.0 degree as in Figure 2 (a), it became wider and wider as the angle increased, then it was plate-shaped at 29.9 degree as in Figure 2 (f). It was confirmed from the above observation that the "Nano Inclusion" remained within the single $LiMn_2O_4$

crystal for every tilting angle. Therefore, it is described that the “Nano Inclusion” was plate-shaped and completely placed within the single $LiMn_2O_4$ crystal.

HAADF-STEM images and electron diffraction patterns for the samples of x=0.02 and 0.05 are shown in Figure 3 (a) to 3 (h). Figure 3 (b), 3 (c), and 3 (d) show electron diffraction patterns at points 1, 2, 3 of Figure 3 (a) for x = 0.02, respectively. Point 1 and 3 belong to the gray area which is identified as $LiMn_2O_4$. The electron diffraction patterns of point 1 and 3 are very similar to each other indicating that both the atomic arrangement and the orientation at the points is the same. Point 2 belongs to the white line which is identified as the “Nano Inclusion”. The electron diffraction pattern of point 2 is very similar to those of point 1 and 3. Figure 3 (f), 3 (g), and 3 (h) show electron diffraction patterns at point 4, 5, 6 of Figure 3 (e) for x = 0.05, respectively. Point 4 and 6 belong to the area indicated as $LiMn_2O_4$. The electron diffraction pattern of points 4 and 6 are similar to each other. Point 5 belongs to the white line area indicated as a “Nano Inclusion”. The electron diffraction pattern of point 5 is very similar to those of point 4 and 6. These above results indicate that the electron diffraction patterns of “Nano Inclusions” are similar to those of the surrounding $LiMn_2O_4$. This means that both the atomic arrangement and the orientation of the “Nano Inclusion” is similar to those of the surrounding $LiMn_2O_4$. It is considered that the “Nano Inclusion” is connected to the $LiMn_2O_4$ matrix without forming a grain boundary.

The lattice parameters are a=0.82476 nm for $LiMn_2O_4$ with cubic spinel structure on JCPDS No. 35-0782 and a=b=0.5720 nm, c=0.9245 nm for $ZnMn_2O_4$ with tetragonal spinel structure on JCPDS No. 24-1133. When the tetragonal I lattice is changed to the tetragonal F lattice, it is calculated that the lattice parameter is a'=b'=0.809 nm, c'=0.9245 nm for $ZnMn_2O_4$. The value of a for $LiMn_2O_4$ is close to those of a'= b' for $ZnMn_2O_4$. Figure 4 shows a schematic atomic arrangement of the projection view for the (100) plane of $LiMn_2O_4$ and the (110) plane of $ZnMn_2O_4$. The atomic arrangement of $LiMn_2O_4$ along the <100> direction is very similar to that of $ZnMn_2O_4$ along the [110] or $[1\bar{1}0]$ direction. The {100} planes of $LiMn_2O_4$ and the (110) or $(1\bar{1}0)$ plane of $ZnMn_2O_4$ have a common cubic close-packed oxygen arrangement as shown in Figure 4. It is considered that such a close lattice match and a common cubic close-packed oxygen arrangement allow these planes to connect to each other with a high affinity. Taking the HAADF-STEM images of Figure 2 into consideration, it is concluded that $ZnMn_2O_4$ spreads widely along these directions. Meanwhile, the value of a for $LiMn_2O_4$ is different from that of c' for $ZnMn_2O_4$. Also, The close-packed oxygen arrangement of $LiMn_2O_4$ along the <100> direction and that of $ZnMn_2O_4$ along the [001] direction are quite different from each other as shown in Figure 4. It is considered that such a mismatched lattice parameter and the quite different oxygen arrangement prevent $ZnMn_2O_4$ from growing into the $LiMn_2O_4$ matrix.

Figure 5 (a) shows a HAADF-STEM image for the sample of x =0.05 and Figure 5 (b) represents the HRTEM image in the selected area marked by a square in Figure 5 (a). As shown in Figure 5 (b), it is indicated that the $LiMn_2O_4$ area and the "Nano Inclusion" area are well-recognized at an atomic scale, that the atomic arrangement is continuously connected, and that there is no grain boundary. Figure 5 (c) shows the corresponding fast Fourier transform (FFT) pattern taking from area 1($LiMn_2O_4$). The d-spacings derived from this FFT pattern can be well assigned to the 022, 004, and 040 diffraction spots of $LiMn_2O_4$ on JCPDS No. 35-0782 as indicated in Figure 5 (c). The indexes of Figure 5 (c) can be interpreted as electron diffraction patterns for the (100) plane of $LiMn_2O_4$. Figure 5 (d) shows the corresponding FFT pattern taking from area 2($ZnMn_2O_4$). The d-spacings derived from FFT pattern can be well attributed to the $\bar{1}12$, $\bar{2}20$, 004, and $\bar{2}24$ diffraction spots of $ZnMn_2O_4$ on JCPDS No. 24-1133 as indicated in Figure 5 (d). The indices of Figure 5 (d) can be interpreted as the electron diffraction pattern for the (110) plane of $ZnMn_2O_4$. Figure 5 (d) shows the FFT pattern for the (110) plane of $ZnMn_2O_4$. Figure 5 (b) indicates that the (100) plane of $LiMn_2O_4$ and the (110) plane of $ZnMn_2O_4$ are observed. The HRTEM image and the FFT patterns revealed the (100) plane of $LiMn_2O_4$ and the (110) plane of $ZnMn_2O_4$, which matched with the above mentioned lattice parameter and oxygen arrangement model well. The (100) plane of $LiMn_2O_4$ and the (110) plane of $ZnMn_2O_4$ have a slight mismatched atomic arrangement. At the same time, the (100) plane of $LiMn_2O_4$ and the (001) plane of $ZnMn_2O_4$ have a largely mismatched atomic arrangement. Taking the HAADF-STEM

images of Figure 2 into consideration, “Nano Inclusions” can be considered to have spread widely along particular planes and not along other planes. Therefore, $ZnMn_2O_4$ grew in the $LiMn_2O_4$ matrix widely along the [110] and [$1\dot{1}0$] direction of $ZnMn_2O_4$ with the accompanying slight mismatch, which prevented the $ZnMn_2O_4$ layer from growing thick, therefore the $ZnMn_2O_4$ was shaped into a thin plane or plate within the single $LiMn_2O_4$ crystal. It is concluded that $LiMn_2O_4$ and “Nano Inclusions” connect closely without grain boundaries, that the “Nano Inclusion” was placed within a single $LiMn_2O_4$ crystal, and that “Nano Inclusion” forms as a thin plane plate.

Conclusions

The crystal structure of $LiMn_2O_4$ with “Nano Inclusions” were studied in detail by conventional HAADF-STEM observation, HAADF-STEM observation with the electron beam tilted to the TEM specimen, electron diffraction, HRTEM and the FFT patterns. Observation with the electron beam tilted to the specimen revealed that the “Nano Inclusion” was shaped into a thin plane / plate. The electron diffraction patterns revealed that the “Nano Inclusion” was placed within a single $LiMn_2O_4$ crystal. It was revealed that the (100) plane of $LiMn_2O_4$ and the (110) plane of $ZnMn_2O_4$ connected closely without grain boundaries by HRTEM observation and the corresponding FFT patterns.

References

1. L. Guohua, H. Ikuta, T. Uchida and M. Wakihara, *J. Electrochem. Soc.*, 1996, **143**, 178-182.
2. H. J. Choi, K. M. Lee and J. G. Lee, *J. Power Sources*, 2001, **103**, 154-159.
3. C.H. Shen, R.S. Liu, R. Gundakaram, J.M. Chen, S.M. Huang, J.S. Chen and C.M. Wang, *J. Power Sources*, 2001, **102**, 21-28.
4. C. Sigala, D. Guyomard, A. Verbaere, Y. Piffard and M. Tournoux, *Solid State Ionics*, 1995, **81**, 167-170.
5. A. D. Robertson, S. H. Lu and W. F. Howard, Jr., *J. Electrochem. Soc.*, 1997, **144**, 3505-3512.
6. A. D. Robertson, S. H. Lu, W. F. Averill and W. F. Howard, Jr., *J. Electrochem. Soc.*, 1997, **144**, 3500-3505.
7. Y. Xia and M. Yoshio, *J. Electrochem. Soc.*, 1996, **143**, 825-833.
8. Y. Gao and J. R. Dahn, *J. Electrochem. Soc.*, 1996, **143**, 100-114.
9. J. M. Tarascon, E. Wang, F. K. Shokoohi, W, R. McKinnon and S. Colson, *J. Electrochem. Soc.*, 1991, **138**, 2859-2864.
10. A. de Kock, E. Ferg and R.J. Gummow, *J. Power Sources*, 1998, **70**, 247-252.
11. F. Le Cras, D. Bloch, M. Anne and P. Strobel, *Solid State Ionics*, 1996, **89**, 203-213.
12. R.J. Gummow, A. de Kock and M.M. Thackeray, *Solid State Ionics*, 1994, **69**, 59-67.
13. S. Guo, X. He, W. Pu, Q. Zeng, C. Jiang and C.Wan, *Int. J. Electrochem. Sci.*, 2006, **1**, 189-193.

14. Y.-K. Sun, K.-J. Hong and J.Prakash, *J. Electrochem. Soc.*, 2003, **150**, A970-A972.

15. S.-W. Lee, K.-S. Kima, H.-S. Moon, H.-J. Kim, B.-W. Cho, W.-I. Cho, J.-B. Ju and J.-W. Park, *J. Power Sources*, 2004, **126**, 150-155.

16. A. Eftekhari, *Solid State Ionics*, 2004, **167**, 237-242.

17. G.G. Amatucci, A. Blyr, C. Sigala, P. Alfonse and J.M. Tarascon, *Solid State Ionics*, 1997, **104**, 13-25.

18. N. Ozawa, K. Donoue and T. Yao, *Electrochem. Solid-State Lett.*, 2003, **6**, A106-A108.

19. M. Hibino, M. Nakamura, Y. Kamitaka, N. Ozawa and T. Yao, *Solid State Ionics*, 2006, **177**, 2653-2656.

20. S. Esaki, M. Nishijima and T. Yao, *ECS Electrochem. Lett.*, 2013, **2**, A93-A97 (2013).

21. H. Wang, Y.-I. Jang, B. Huang, D. R. Sadoway and Y.-M. Chiang, *J. Electrochem. Soc.*, 1999, **146**, 473-480.

22. Toray Research Center, Inc. Japan, TRC poster sessions 2003 VII-1, "Crystal Analysis for Cathode Materials of Lithium Ion Batteries", Tokyo, 2003.

23. D. Wang, X. Wu, Z. Wang and L. Chen, *J. Power Sources*, 2005, **140**, 125–128.

24. H. Gabrisch, J. Wilcox and M. M. Doeff, Electrochem. Solid-State Lett., 2008, 11, A25-A29.

25. K. Momma and F. Izumi, *J. Appl. Cryst.*, 2011, **44**, 1272-1276.

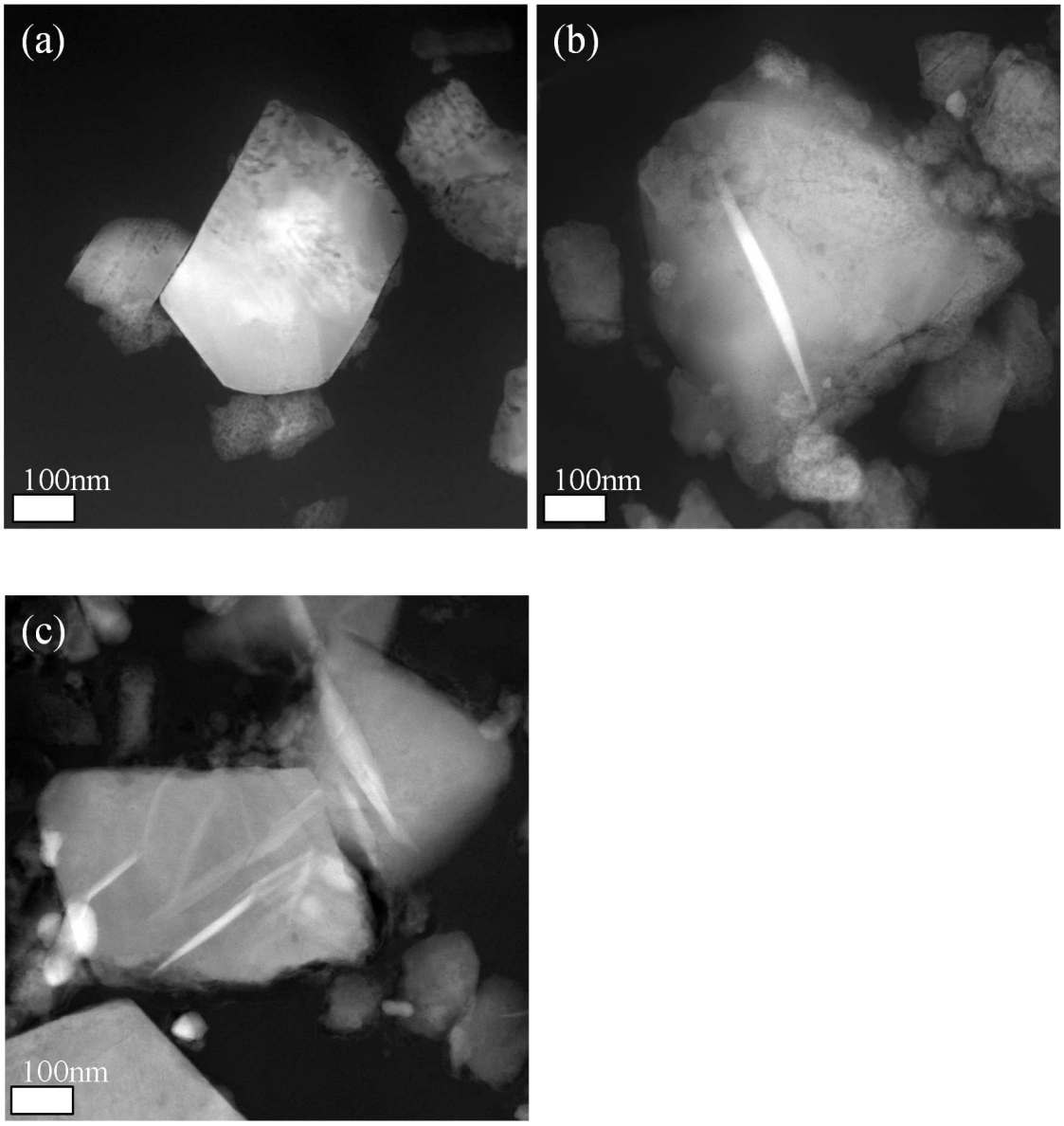

Figure 1

HAADF-STEM images of the samples: (a) $x = 0$, (b) $x = 0.02$, (c) $x = 0.05$.

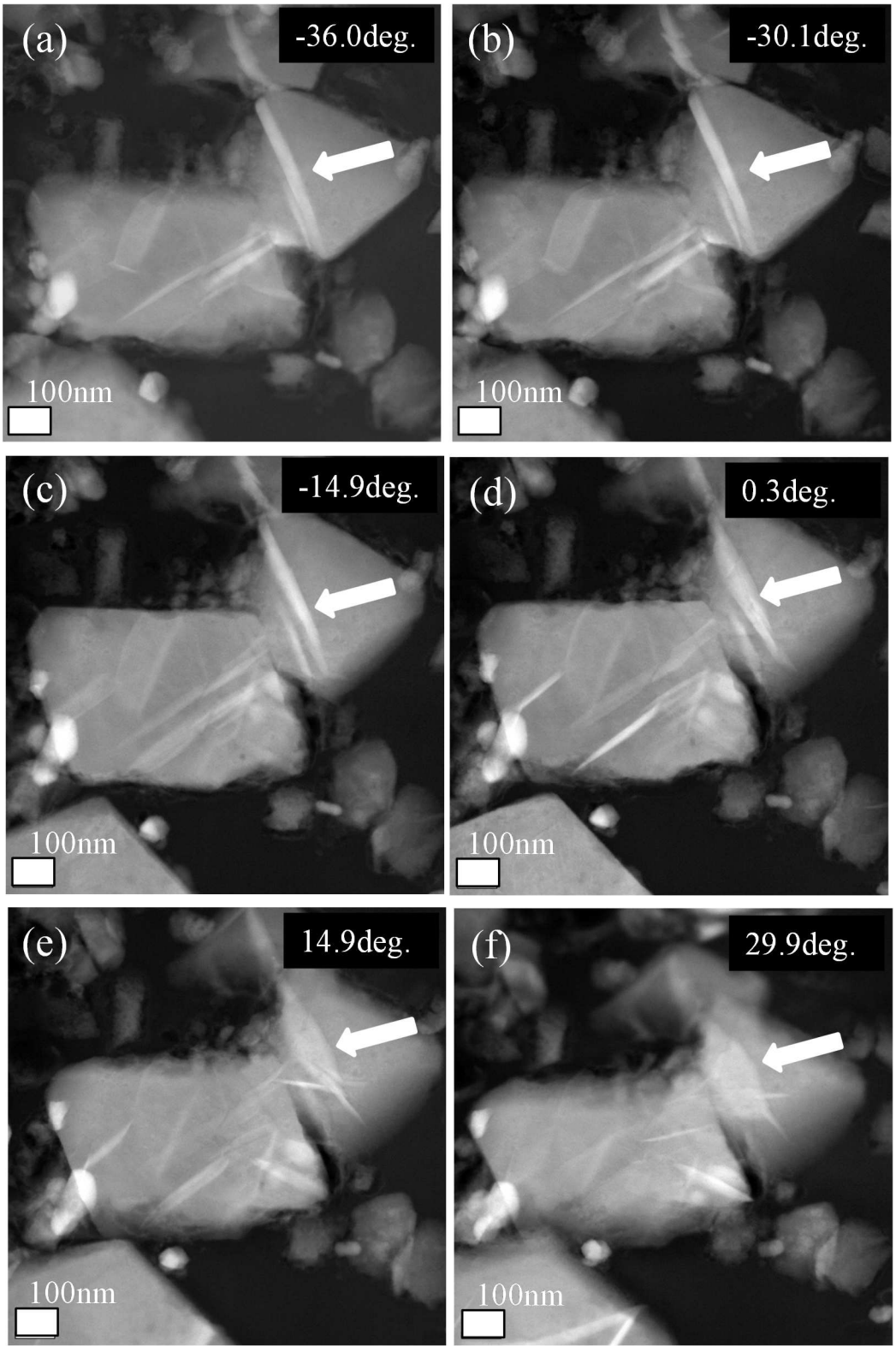

Figure 2

HAADF-STEM images with electron beam tilted to the specimen of the x = 0.05 sample.

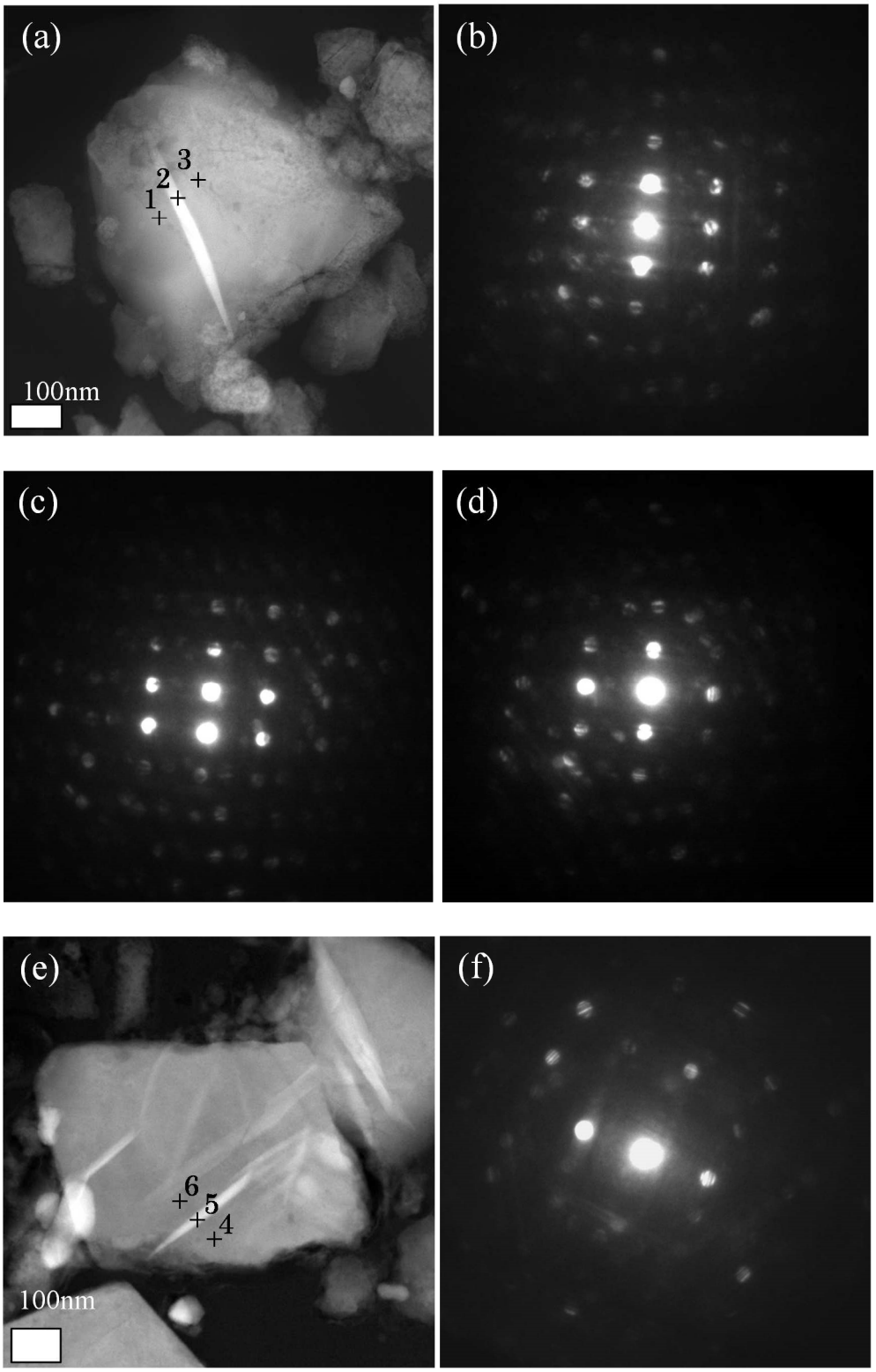

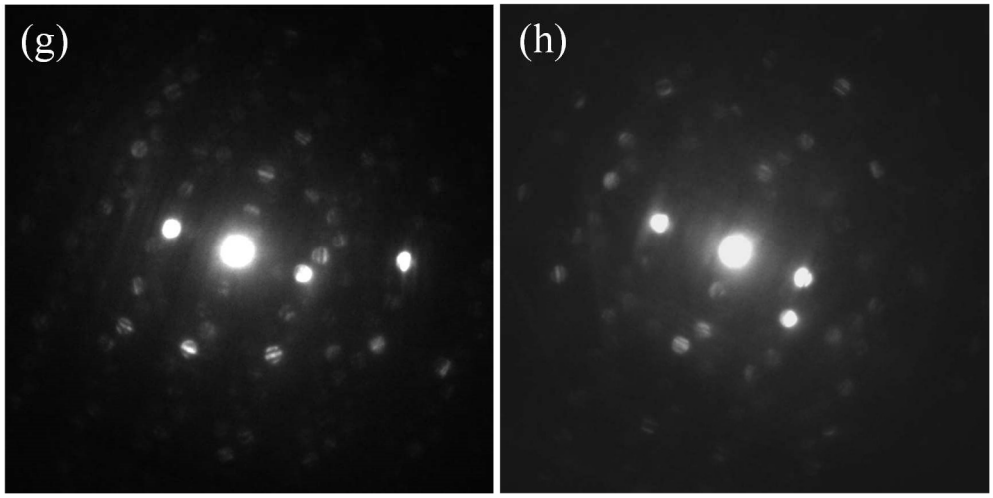

Figure 3

Electron diffraction patterns for the sample of x = 0.02 and 0.05: A HAADF-STEM image of x =0.02 is Figure 3 (a). Figure 3 (b), 3 (c), and 3 (d) are electron diffraction patterns at point 1, 2, 3 of Figure 3 (a), respectively. A HAADF-STEM image of x =0.05 is Figure 3 (e). Figure 3 (f), 3 (g), and 3 (h) are electron diffraction patterns at point 4, 5, 6 of Figure 3(e), respectively.

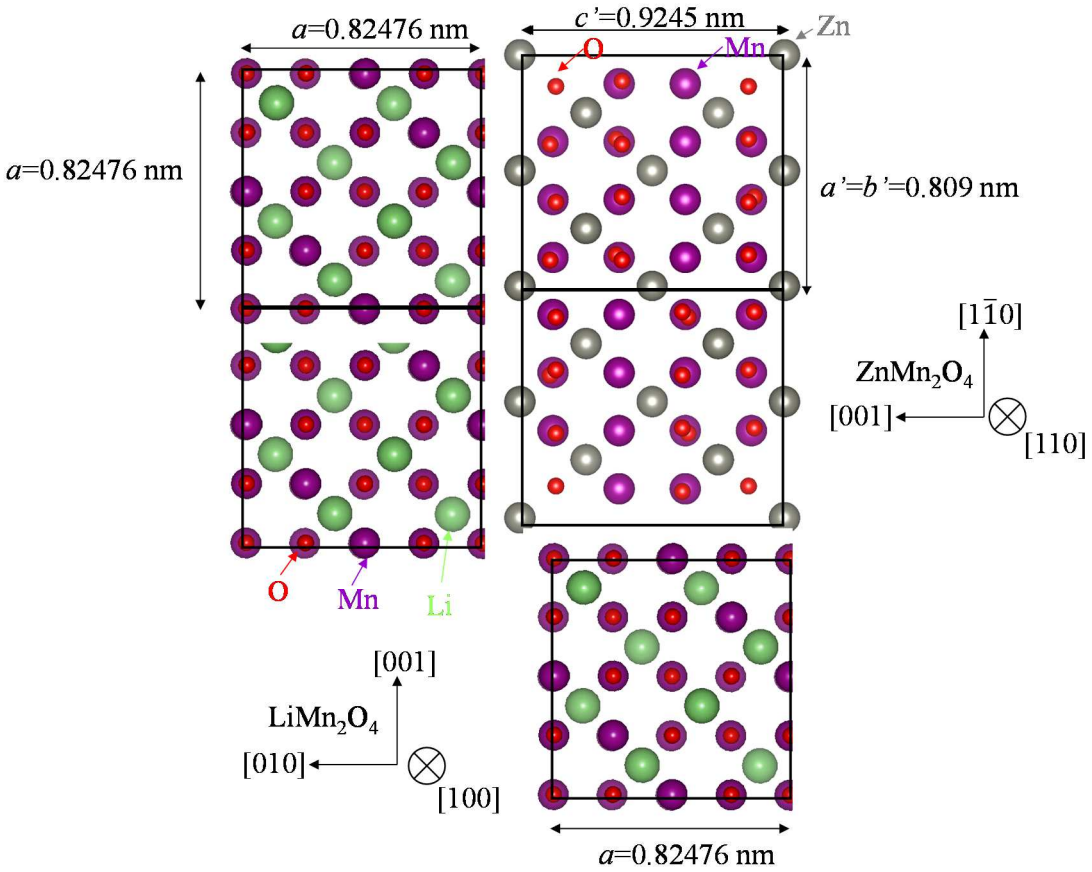

Figure 4

A schematic atomic arrangement of the (100) plane of $LiMn_2O_4$ and the (110) plane of $ZnMn_2O_4$. The black solid line shows the unit cell of $LiMn_2O_4$ or $ZnMn_2O_4$. Upper left and lower right figures show the projection view of the (100) plane of $LiMn_2O_4$. The upper right figure shows the projection view of the (110) plane of $ZnMn_2O_4$. The structures were drawn using VESTA software.[25]

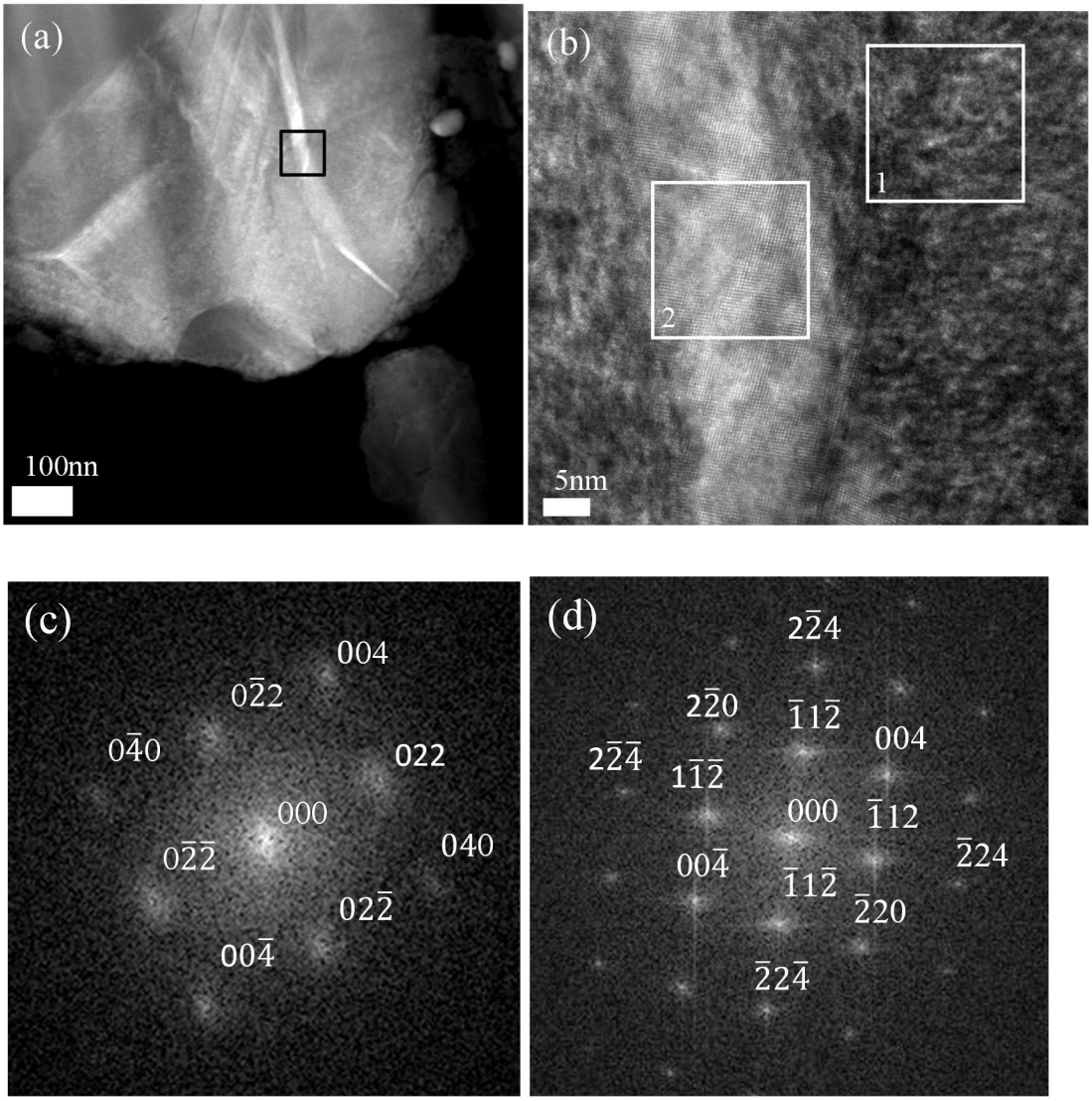

Figure 5

HAADF-STEM image, HRTEM image and the FFT patterns of the x = 0.05 sample:(a) a HAADF-STEM image, (b) HRTEM image, (c) and (d) the corresponding FFT patterns taking from area 1 and 2.